The Journal of Biological Chemistry
AFFINITY SITES

Cell Biology:
Calcyon Forms a Novel Ternary Complex with Dopamine D $_1$ Receptor through PSD-95 Protein and Plays a Role in Dopamine Receptor Internalization

CELL BIOLOGY
NEUROBIOLOGY

Chang Man Ha, Daehun Park, Jeong-Kyu Han, June-ill Jang, Jae-Yong Park, Eun Mi Hwang, Heon Seok and Sunghoe Chang
J. Biol. Chem. 2012, 287:31813-31822.
doi: 10.1074/jbc.M112.370601 originally published online July 26, 2012

THE JOURNAL OF BIOLOGICAL CHEMISTRY VOL. 287, NO. 38, pp. 31813–31822, September 14, 2012

Calcyon Forms a Novel Ternary Complex with Dopamine D_1 Receptor through PSD-95 Protein and Plays a Role in Dopamine Receptor Internalization*[S]

Received for publication, April 9, 2012, and in revised form, June 5, 2012 Published, JBC Papers in Press, July 26, 2012, DOI 10.1074/jbc.M112.370601

Chang Man Ha[‡§¶1], Daehun Park[‡], Jeong-Kyu Han[‡], June-ill Jang[‖], Jae-Yong Park[‡‡], Eun Mi Hwang[‡‡], Heon Seok[§§], and Sunghoe Chang[‡§¶ ¶¶2]**

From the [‡]Departments of Physiology and Biomedical Sciences, [§]Neuroscience Research Institute, Medical Research Center, [¶]Biomembrane Plasticity Research Center, and [¶¶]Bio-Max Institute, Seoul National University College of Medicine, Seoul 110-799, the [‖]School of Nano-Bioscience and Chemical engineering, Ulsan National Institute of Science and Technology, Ulsan 689-798, the [**]Department of Physiology, Institute of Health Science, and Medical Research Center for Neural Dysfunction, Biomedical Center (BK21), Gyeongsang National University School of Medicine, Jinju 660-751, the [‡‡]Center for Functional Connectomics, Korea Institute of Science and Technology (KIST), Seoul 136-791, and the [§§]Department of Biomedical Engineering, Jungwon University, Goesan-gun, Chungcheongbuk-do Korea 367-805

Background: Calcyon has been associated with various dopamine D_1 receptor signalings despite no direct interaction between them.
Results: Calcyon forms a novel ternary complex with D_1DR through PSD-95.
Conclusion: Calcyon, by forming a ternary complex, regulates D_1DR internalization in a phosphorylation-dependent manner.
Significance: Regulation of dopaminergic signaling by calcyon·PSD-95·D_1DR complex may represent a novel target for related neuropsychiatric disorders.

Calcyon, once known for interacting directly with the dopamine D_1 receptor (D_1DR), is implicated in various neuropsychiatric disorders including schizophrenia, bipolar disorder, and attention deficit hyperactivity disorder. Although its direct interaction with D_1DR has been shown to be misinterpreted, it still plays important roles in D_1DR signaling. Here, we found that calcyon interacts with the PSD-95 and subsequently forms a ternary complex with D_1DR through PSD-95. Calcyon is phosphorylated on Ser-169 by the PKC activator phorbol 12-myristate 13-acetate or by the D_1DR agonist SKF-81297, and its phosphorylation increases its association with PSD-95 and recruitment to the cell surface. Interestingly, the internalization of D_1DR at the cell surface was enhanced by phorbol 12-myristate 13-acetate and SKF-81297 in the presence of calcyon, but not in the presence of its S169A phospho-deficient mutant, suggesting that the phosphorylation of calcyon and the internalization of the surface D_1DR are tightly correlated. Our results suggest that calcyon regulates D_1DR trafficking by forming a ternary complex with D_1DR through PSD-95 and thus possibly linking glutamatergic and dopamine receptor signalings. This also raises the possibility that a novel ternary complex could represent a potential therapeutic target for the modulation of related neuropsychiatric disorders.

As a brain-specific protein, calcyon is mainly localized in the intracellular endosomal vesicles of dendritic spines in D_1DR[3]-expressing pyramidal cells in the prefrontal cortex and hippocampus and dorsal striatum region (1, 2). Initially, calcyon had been reported as a D_1DR-interacting protein (DRIP), but later studies revealed that there was no direct interaction between calcyon and D_1DR (3). Recent studies, however, have introduced calcyon as a candidate gene for D_1DR-related neurophysiological disorders. Calcyon levels were elevated in schizophrenia patients (4, 5), whereas calcyon transgenic mice showed reduced anxiety and an impaired working memory (6, 7). Calcyon was up-regulated in the rodent model of attention deficit hyperactivity disorder (8), and its gene variations are known to be associated with cocaine dependence (9). In addition, calcyon is known to potentiate cross-talk between $G\alpha_s$-linked D_1DR and heterologous $G_{q/11}$-coupled receptors. When primed with agonists to $G_{q/11}$-coupled receptors, calcyon induces D_1DR to stimulate intracellular Ca^{2+} release (2, 10). Therefore, all of the above results suggest a possible functional interaction between calcyon and D_1DR despite no direct interaction between them. Indeed, a recent study suggested that calcyon-containing vesicles might transport D_1DR by associat-

* This work was supported by Basic Science Research Program Grant 2010-0022375 from the National Research Foundation (NRF) of Korea (to C. M. H.) funded by the Ministry of Education, Science and Technology (MEST), Republic of Korea. Research was also supported by grants from the NRF of Korea (SRC 20100029395) (to S. C.) funded by the MEST, Republic of Korea.
[S] This article contains supplemental Figs. 1–6.
1 To whom correspondence may be addressed: Dept. of Biomedical Sciences, Seoul National University College of Medicine, 314 Biomedical Science Bldg., 28 Yeongeon-dong, Jongno-gu, Seoul 110-799, Korea. Tel.: 82-2-3668-7659; Fax 82-2-3673-2167; E-mail: gkckdaks@snu.ac.kr.
2 To whom correspondence may be addressed: Dept. of Physiology, Seoul National University College of Medicine, 309 Biomedical Science Bldg., 28 Yeongeon-dong, Jongno-gu, Seoul 110-799, South Korea. Tel.: 82-2-740-8918; Fax 82-2-3673-2167; E-mail: sunghoe@snu.ac.kr.

3 The abbreviations used are: D_1DR, dopamine D_1 receptor; PSD, postsynaptic density; SH3, Src homology 3; BiFC, bimolecular fluorescence complementation; PMA, phorbol 12-myristate 13-acetate; EGFP, enhanced green fluorescent protein; Lca, clathrin light chain; RIPA, radioimmune precipitation; a.a., amino acids; ANOVA, analysis of variance; HSD, honestly significant difference; DMSO, dimethyl sulfoxide.

ing calcyon with D_1DR through their assembly to clathrin (11). However, as a single transmembrane protein, it is not clear how calcyon can regulate the internalization of D_1DR from the plasma membrane to endocytic vesicles.

PSD-95 is prominently expressed in postsynaptic densities (PSDs) and is a prototypical scaffolding protein with multiple protein interaction domains: NH_2-terminus, Discs large/zona occludens-1 (PDZ), SH3 (Src homology 3), and guanylate kinase-like domains (12). It forms the backbone of the postsynaptic protein complex that organizes receptors and signal transduction molecules, enabling the functional effects of the receptors at PSDs. PSD-95 is known to regulate D_1DR signaling and the formation of the D_1DR-associated protein·protein complex (13, 14). The NH_2 terminus of PSD-95 interacts with the carboxyl-terminal tail of D_1DR and facilitates constitutive D_1DR internalization as well as internalization of the NMDA receptor, which complexes with D_1DR, thus linking dopamine signaling and glutamatergic signaling (15).

Here, we show that calcyon interacts with PSD-95. This interaction formed a ternary protein complex containing calcyon·PSD-95 and D_1DR in the dendritic spines of hippocampal neurons. Furthermore, we found that calcyon was phosphorylated on the Ser-169 residue through a PKC-dependent pathway. Phosphorylation of calcyon strongly enhanced its interaction with PSD-95, increased its surface localization, and consequently induced the internalization of the surface D_1DR.

EXPERIMENTAL PROCEDURES

Constructs—To construct expression vectors for calcyon, rat full-length calcyon cDNA (accession number: AF303658) was extracted by PCR from rat brain cDNA library and inserted into target vectors (EGFP-C1, pCDNA3-HA, and C-terminal FLAG-tagged pFLAG-CMV (Sigma). Serine phosphorylation site of calcyon (S169A) was generated by site-directed point mutations using the QuikChange® site-directed mutagenesis kit (Stratagene. Austin, TX). Full-length rat PSD-95 (accession number: P31016) was amplified by PCR and subcloned into pCDNA3-HA and EGFP-N1 vectors (Invitrogen). The HA-D_1DR was kindly provided by Dr. Wei-Dong Yao (Harvard University), and all DNA constructs were verified by DNA sequencing. These expression vectors were transfected into HEK293T, SH-SY5Y cells, and neurons for Western blot and imaging analysis.

Coimmunoprecipitation and Immunoblotting—To verify the interaction of calcyon with PSD-95, adult rat brain was homogenized with a modified RIPA buffer (50 mM Tris-HCl pH 7.5, 5 mM EDTA, 150 mM NaCl, 1% Nonidet P-40, 1 mM sodium orthovanadate, 1 mM PMSF, 10 mM leupeptin, 1.5 mM pepstatin, and 1 mM aprotinin) (16) and incubated with anti-calcyon antibody for immunoprecipitation (Santa Cruz Biotechnology, Santa Cruz, CA) and for immunoblotting (Abcam, Cambridge, MA). Mouse anti-PSD-95 monoclonal antibody and rabbit anti-PSD-95 polyclonal antibody were from NeuroMab (Davis, CA) and Synaptic Systems (Göttingen, Germany), respectively. HEK293T cells were cotransfected with FLAG-calcyon, PSD-95-EGFP, and HA-D_1DR, and the cells were washed twice with cold PBS and extracted at 4 °C with a modified RIPA buffer. The mixtures were then incubated with 30 μl of protein A-Sepharose (50% slurry) for 1 h, pelleted by centrifugation, and analyzed by SDS-PAGE (8–15% gels). Proteins on gels were transferred to PVDF membranes (Pall Life Sciences, Ann Arbor, MI), and the membranes were incubated with anti-calcyon (1:800), anti-D_1DR (1:1,000), or anti-PSD-95 (1:2,000) primary antibodies for 1 h at room temperature or overnight at 4 °C. Immunoblot was performed with anti-HA antibody (1:1000; Covance, Princeton, NJ), anti-FLAG (1:1,000; Sigma), or anti-GFP (1:3,000; GeneTex, Irvine, CA). The immunoreactions were detected with SuperSignal West Pico chemiluminescent substrate (Thermo Scientific). After chemiluminescence detection using an ImageQuant LAS 4000 (GE Healthcare, Uppsala, Sweden), images were analyzed using the ImageJ software.

To identify the endogenous ternary complex of calcyon·PSD-95·D_1DR, cultured hippocampal neuron lysates (days *in vitro* 16) were prepared after treatment of SKF-81297 (10 μM) for 15 min and harvested with modified RIPA buffer. They were then clarified by centrifugation at 15,000 × *g* for 30 min. Protein concentrations were measured using a BCA assay (Pierce).

The 800–1500 μg of lysates were incubated with 20 μl of protein A-Sepharose 4 Fast Flow (GE Healthcare) for 1 h at 4 °C to remove nonspecific proteins and reincubated with anti-calcyon, anti-PSD-95 (Synaptic Systems), or anti-D_1DR (Santa Cruz Biotechnology) antibodies overnight at 4 °C. To test the roles of phosphorylation of calcyon, EGFP-calcyon transfected HEK293T cells and FLAG-calcyon·PSD-95-EGFP·HA-D_1DR cotransfected HEK293T cells were incubated with 1 μM PMA (Sigma) and 10 μM SKF-81297 (Santa Cruz Biotechnology), respectively. Cell lysates were incubated with anti-GFP (GeneTex) or anti-FLAG (Sigma) antibody and immunoblotted with anti-phospho-serine antibody (Acris Antibodies GmbH, Herford, Germany).

GST Pulldown Assays—Full-length rat PSD-95 (1–724), N terminus (1–64 amino acids), PDZ1–3 (65–393 amino acids), PDZ1 (65–151 amino acids), PDZ2 (160–246 amino acids), PDZ3 (313–393 amino acids), ΔSH3 (lacking amino acids 428–498), and SH3 (428–498 amino acids) of PSD-95, full-length rat calcyon (1–226 amino acids), extracellular region (1–88 amino acids), C terminus (109–226 amino acids), and the 175–226-amino acid part of the C terminus (C-End) of calcyon were amplified by PCR and subcloned into pGEX4T-1 for the GST pulldown assays. PCR products of calcyon (175–200 and 201–226) were subcloned into pDESTc15 vector (Invitrogen) using the Gateway cloning system (Invitrogen). The plasmids were transformed into BL-21, and the transformants were cultured in 2× YT medium supplemented with ampicillin. After a 5-h induction with 0.5 mM isopropyl 1-thio-β-D-galactopyranoside at 30 °C, the cultures were sonicated in lysis buffer (1% Triton X-100, 0.5% sodium deoxycholate, 20 mM Tris, pH 8.0, 150 mM NaCl, 1 mM $MgCl_2$, 1 mM EGTA, 0.1 mM PMSF) and centrifuged at 15,000 × *g* for 15 min, and the supernatants were incubated with glutathione-agarose-4B beads (GE Healthcare) for 1 h at 4 °C. After washing three times with lysis buffer, the beads were incubated for 2 h at 4 °C or overnight with brain lysates in lysis buffer. The beads were then washed extensively with lysis buffer and analyzed by SDS-PAGE and immunoblotting.

In Vitro Phosphorylation Assay—The 156–206-a.a domains of calcyon (P-WT) and S169A mutant (P-SA) were cloned into pDEST15 vector using the Gateway cloning system and transformed to BL-21. The *Escherichia coli* was sonicated with lysis buffer (1% Triton X-100, 0.5% sodium deoxycholate, 20 mM Tris, 150 Mm NaCl, 1 mM $MgCl_2$, 1 mM EGTA, PH 7.2, 0.1 mM PMSF). The phosphorylation of wild type (P-WT) and phospho-mutant S169A (P-SA) was performed using glutathione-Sepharose 4B resin (GE Healthcare). For the *in vitro* phosphorylation assay, 25 μg of purified GST-P-WT and GST-P-SA were incubated with 20 ng of PKC-catalytic subunit (Millipore, Billerica, MA) in PKC assay dilution buffer II with 2 mM Mg^{2+}-ATP containing phosphatase inhibitor mixture III (Sigma) at 30 °C for 40 min. The reaction was stopped by adding 10 mM EDTA and centrifuged at 1000 × *g* for 1 min, and the supernatant was removed. 2× SDS-Laemmli buffer was added without washing followed by SDS-PAGE. P-WT phosphorylation was detected by immunoblotting with phospho-serine antibody (Acris Antibodies GmbH).

cAMP Enzyme Immunoassay—HEK293T cells were transiently transfected with FLAG-calcyon, PSD-95-EGFP, and HA-D_1DR using Lipofectamine 2000 (Invitrogen) and grown for 27 h in complete DMEM medium and then serum-starved for 16 h before SKF-81297 treatment. The cells were stimulated by 10 μM SKF-81297 for 30 min, and cAMP accumulation was measured with a cAMP direct immunoassay kit (Abcam). In brief, DMEM was removed from the plate, and cells were washed with warmed 1× Dulbecco's PBS briefly and incubated with 0.1 M HCl at room temperature for 20 min. Cells were dissociated by pipetting up and down, neutralizing buffer and acetylation reagent mixture were added to the cell lysates (>1 μg/μl concentration), and reaction mixtures were incubated at room temperature for 10 min. Each acetylated sample and standards were transferred to a protein G-coated white 96-well plate. Rabbit anti-cAMP polyclonal antibody was added to standard, and samples and reaction mixtures were incubated for 1 h at room temperature, reincubated with cAMP-HRP for 1 h, washed, and developed with the HRP developer for 1 h. The reaction was stopped by adding 1 M HCl and read the plate at an optical density of 450 nm.

Cell Culture, Immunocytochemistry, and Image Acquisition—HEK293T and SH-SY5Y cells were cultured at 37 °C and 5% CO_2 in Dulbecco's modified Eagle's medium (Invitrogen) supplemented with 10% fetal bovine serum (HyClone, Logan, UT). Transfection was carried out using Lipofectamine 2000 (Invitrogen), and cells were observed after 24–36 h. The confocal images were acquired with an Olympus FV 1000 using a sequential scan tool mounted on an Olympus IX-81 microscope fitted with a 100×/1.4 NA objective lens driven by Olympus FluoView software. For immunocytochemistry, cells were fixed in 4% formaldehyde with 4% sucrose in PBS for 15 min, permeabilized for 5 min in 0.25% Triton X-100, PBS, and blocked for 30 min in 10% BSA, PBS at 37 °C. The cells were incubated with primary antibodies in 3% BSA, PBS for 2 h at 37 °C or overnight at 4 °C, washed in PBS, and incubated with secondary antibodies in 3% BSA, PBS for 45 min at 37 °C. For colocalization experiments with calcyon, PSD-95 and D_1DR, primary cultured neurons were permeabilized with 0.25% Triton X-100 for 5 min at room temperature before primary antibodies. Analysis and quantification of data were performed with MetaMorph software (Molecular Devices, Sunnyvale, CA) and SigmaPlot 8.0 (Systat Software, Point Richmond, CA), and data are presented as means ± S.E.

Neuron Culture and Transfection—Experiments were performed in accordance with guidelines set forth by the Seoul National University Council Directive for the proper care and use of laboratory animals. Hippocampal neurons derived from E-18 primary rats were prepared as described (17). Briefly, hippocampi were dissected, dissociated with papain, and triturated with a polished half-bore Pasteur pipette. The cells (2.5×10^5) in minimum Eagle's medium supplemented with 0.6% glucose, 1 mM pyruvate, 2 mM L-glutamine, 10% fetal bovine serum, and antibiotics were plated on poly-D-lysine-coated glass coverslips in a 60-mm Petri dish. Four hours after plating, the medium was replaced with basal media Eagle's (Invitrogen) supplemented with 2% B-27, 10 mM HEPES, and 0.5 mM pyruvate or Neurobasal medium (Invitrogen) supplemented with 2% B-27, 0.5 mM L-glutamine. 4 μM 1-β-D-cytosine-arabinofuranoside (Ara-C, Sigma) was added as needed. Neurons were transfected using the calcium phosphate method (18).

Bimolecular Fluorescence Complementation (BiFC) Assays—For BiFC assays, the full-length cDNAs corresponding to the rat calcyon, C-terminal end (175–200 a.a, 201–226 a.a) of calcyon, and rat PSD-95 were cloned into pDONR207 vectors using the Gateway cloning system (Invitrogen). Next, using LR Clonase (Invitrogen), these entry clones were converted into pDS_XB-VN and pDS_VN-XB or pDS_VC-XB and pDS_XB-VC destination vectors. After sequence verification, SH-SY5Y cells were transfected with various BiFC pairs (1:1 ratio) using Lipofectamine 2000 (Invitrogen). Cells were fixed 12–16 h after transfection with 4% paraformaldehyde and imaged using a confocal microscope (FV-1000, Olympus).

Surface Biotinylation—After 36 h of transfection, biotinylation of cell surface proteins was performed using the cell surface protein isolation kit (Thermo scientific) according to the manufacturer's instructions. Briefly, HEK293 cells grown on 100-mm plates were washed once with ice-cold PBS and incubated with 0.25 mg/ml EZ-Link® Sulfo-NHS-SS-Biotin in PBS for 30 min at 4 °C. The cells were rinsed in quenching solution with Tris-buffered saline to remove free biotin reagents and lysed in lysis buffer. After centrifugation, supernatants were incubated with 50 μl of 50% slurry of immobilized NeutrAvidin for 3 h at 4 °C. Reaction complexes were washed three times with wash buffer, and then biotinylated proteins were eluted by incubating at 37 °C for 15 min in SDS sample buffer followed by immunoblotting with an anti-HA antibody (1:1000) to detect D_1DR and anti-calcyon (1:1,000) antibodies.

RESULTS AND DISCUSSION

A previous study showed that calcyon localizes to the dendritic spines of D_1 receptor-expressing pyramidal cells in the prefrontal cortex (2). PSD-95 is a prominent scaffolding protein with multiple protein interaction domains in the dendritic spine (19, 20). Because the subcellular fractionation data in this study showed that calcyon and PSD-95 protein existed in the PSD and had similar expression patterns during the develop-

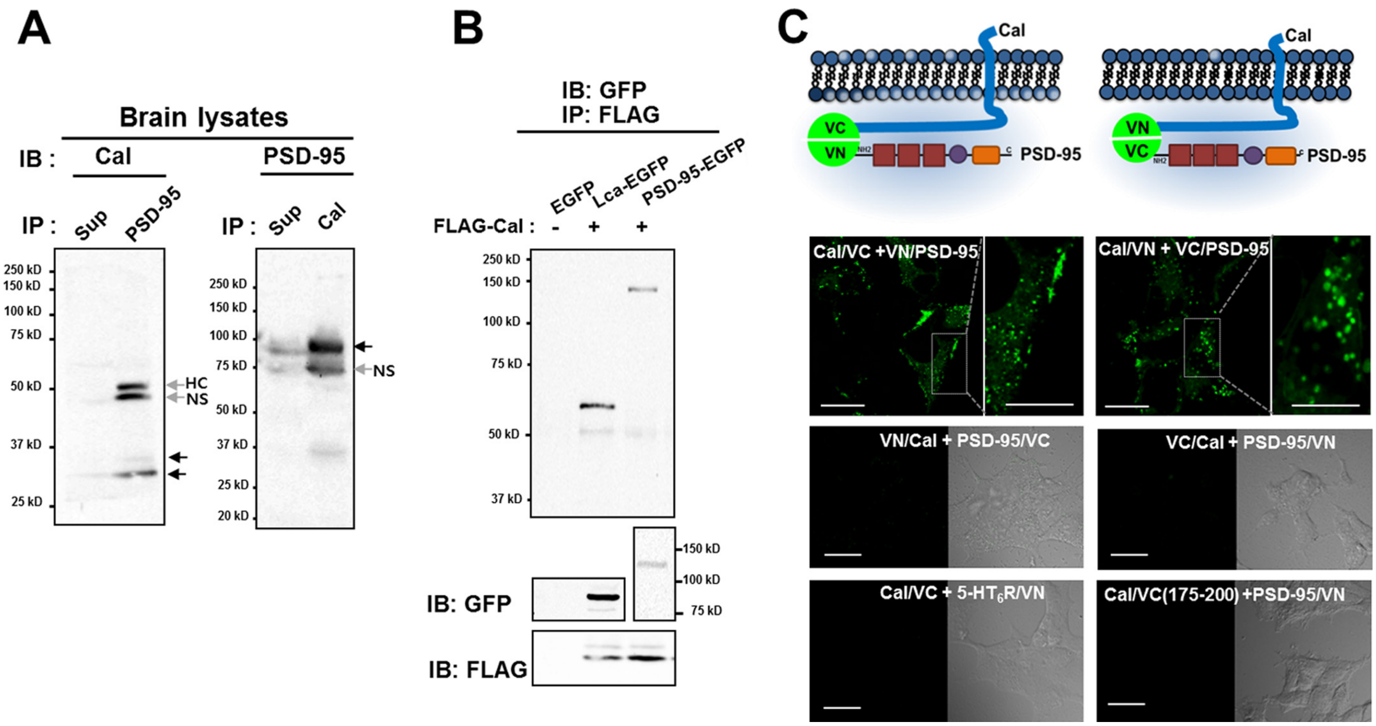

FIGURE 1. **Calcyon associates with PSD-95.** *A*, adult rat brain extracts were immunoprecipitated (*IP*) with mouse monoclonal anti-PSD-95 antibody (*left panel*) or rabbit polyclonal anti-calcyon (*Cal*) antibody (*right panel*) followed by immunoblot (*IB*) analysis with rabbit polyclonal anti-calcyon (*left panel*) or mouse monoclonal anti-PSD-95 antibody (*right panel*). *Arrows* indicate the size of calcyon (*left panel*) and PSD-95 (*right panel*) *NS*; nonspecific band. *HC*; heavy chain. *Sup*; immunoprecipitated supernatants. *B*, HEK293T cells were cotransfected with FLAG-calcyon and EGFP-C_1, PSD-95-EGFP, and Lca-EGFP. Cell lysates were immunoprecipitated with anti-FLAG antibody followed by immunoblotting with anti-GFP antibody. *Lower panel*: the expression of each protein was detected by anti-GFP or anti-FLAG antibody. *C*, schematic figures showing the successful combination of BiFC between calcyon and PSD-95. *Lower panels*: SH-SY5Y cells were cotransfected with various combinations of BiFC pairs. Note that except for the calcyon-VC155·VN173-PSD-95 pair and calcyon-VN173·VC155-PSD-95 pair, all other combinations failed to exhibit a positive fluorescence complementation. *5-HT$_6$R/VN*: 5-HT$_6$ receptor conjugated to VN173. *Cal/VC(175–200)*: calcyon C terminus region (a.a. 175–200) conjugated to VC155. *Scale bar* = 20 μm; 10 μm in *inset*.

ment of rat hippocampal neurons (supplemental Fig. 1), we wondered whether calcyon interacts with PSD-95.

To test this possibility, an immunoprecipitation analysis was performed with adult rat whole brain lysates. Fig. 1 shows that calcyon and PSD-95 coprecipitated, suggesting that they interact with each other endogenously (Fig. 1*A*). When HEK293T cells were cotransfected with FLAG-calcyon, EGFP-C_1 empty vector, clathrin light chain (Lca)-EGFP, and PSD-95-EGFP, calcyon coprecipitated with Lca (*lane 2*) and PSD-95 (*lane 3*) but not with the EGFP empty vector (Fig. 1*B*). This interaction was further confirmed by BiFC assay using the improved yellow fluorescence protein, Venus, which allows for direct visualization of protein interactions at the subcellular sites of their interactions in living cells (21–23). Fluorescence complementation was only observed in a group of cells that coexpressed fragments of Venus (VN173 or VC155) conjugated to the C terminus of calcyon and to the N terminus of PSD-95 (Fig. 1*C*). No complementation was detected when fragments of Venus (VN173 or VC155) were fused to the N terminus of calcyon or the C terminus of PSD-95 (supplemental Fig. 2*A*).

We further investigated which domain of PSD-95 binds to calcyon. A series of GST pulldown assays was done with various domain mutants of PSD-95 and calcyon (Fig. 2, *A* and *B*). Calcyon was found to interact with the full-length PSD-95, the PDZ1–3 domain, and the PDZ1 domain, but not with the N-terminal region, PDZ2, PDZ3, or SH3 domain (Fig. 2*C*). In addition, the full-length PSD-95 and PDZ1 domain of PSD-95 interacted with the C terminus (a.a. 109–226) and C-terminal end (a.a. 175–226) of calcyon, but not with the extracellular region or GST only (Fig. 2*D*). These results suggest that the PDZ1 domain of PSD-95 is responsible for its binding to the C-terminal regions (a.a. 175–226) of calcyon. Although we did not find any consensus binding motif for the class I PDZ domain (X(S/T)X(V/L/I)-COOH) in the C-terminal regions of calcyon, using the PDZ domain-ligand interaction network (PDZNet) and position weight matrices, which contain the experimental data of the PDZ domain-ligand interaction of human PDZ domains (21), we could identify the three putative PDZ binding motifs in the C-terminal regions of calcyon (supplemental Fig. 2*C*). We thus divided the C-terminal regions (a.a. 175–226) into two regions (a.a. 175–200 and a.a. 201–226, respectively) that contained the putative PDZ binding motif(s) and performed a GST pulldown assay. We found that a.a. 201–226 of calcyon strongly bound to PSD-95, whereas a.a. 175–200 did not. This was further supported by the BiFC results in which a group of cells that coexpressed fragments of PSD-95-VN173 or VN173-PSD-95 with the calcyon-VC155 (a.a. 201–226) only showed fluorescent complementation (Fig. 2*E* and supplemental Fig. 2*B*). Because both C-terminal fragments contain the A*XX*V motif, these results indicate that A*XX*V motif does not seem to be involved in PSD-95 binding. To test whether the last four-amino acid sequence (QSPK) of calcyon is the PSD-95 binding motif, we introduced S224A point mutation in the Ser residue of the sequence because Ser/Thr at the −2 position is

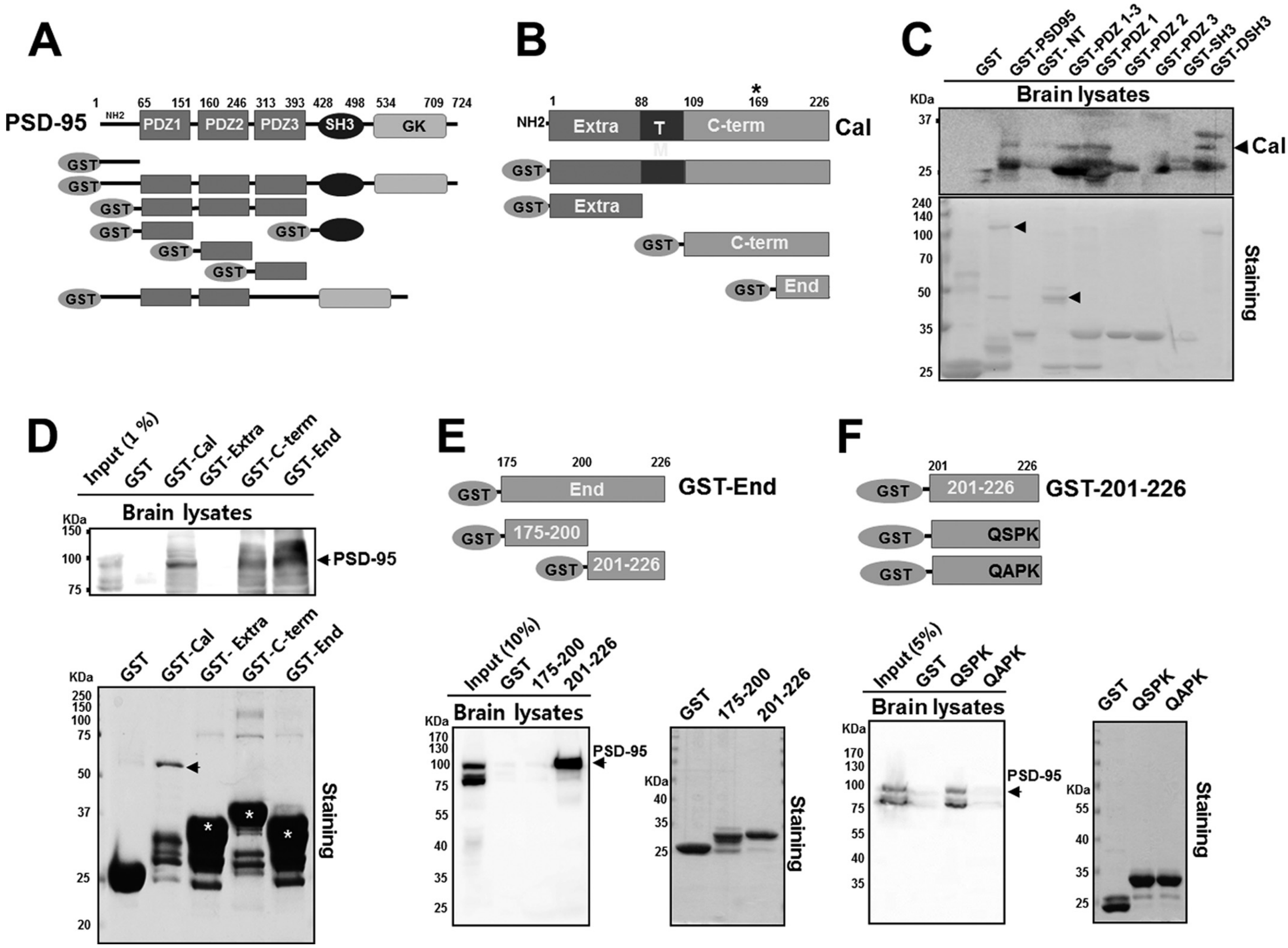

FIGURE 2. **Calcyon interacts with PSD-95.** *A*, schematic figures showing PSD-95 domain structures and each GST-fused domain of PSD-95. *GK*, guanylate kinase-like domain. *B*, schematics of calcyon domain and full-length calcyon (*Cal*) and extracellular region (*Extra*), C terminus (*C-term*), and the 175–226-amino acid part of the C terminus (*End*) of calcyon. *C*, brain lysates were pulled down with GST fusions of PSD-95 full length; N terminus (*NT*); PDZ1–3 domain; PDZ1 domain; PDZ2 domain; PDZ3 domain; SH3 domain lacking amino acids 428–498 (*ΔSH3*); and SH3 domain and GST alone (*DSH3*). The pulldown complex was resolved by SDS-PAGE, and immunoblotting was performed with anti-calcyon antibody (*upper panel*). Calcyon was identified in the full-length GST-PSD-95, GST-PDZ1–3, GST-PDZ1, and GST-ΔSH3 lanes. The expression of GST fusion proteins was identified using Coomassie Blue staining (*lower panel*). *Arrowheads* indicate the purified GST-full-length PSD-95 and PDZ1–3. *D*, adult rat brain lysates were pulled down with GST-fused calcyon, GST-Extra (a.a. 1–226), GST-C-term (a.a. 109–226 of the C terminus), or GST-End (a.a. 175–226), and immunoblotting was performed with anti-PSD-95 antibody (*upper panel*). GST fusion proteins were identified using Coomassie Blue staining (*lower panel*). *Arrowhead* indicates GST-calcyon, and *asterisks* indicate GST fusion proteins. *E*, GST-End of calcyon was divided into two domains (a.a. 175–200 and a.a. 201–226) in which each domain contains one putative PDZ binding motif (See supplemental Fig. 2*C*). Brain lysates were pulled down with each GST fusion protein and immunoblotted with anti-PSD-95 antibody. Note that strong immunoreactivity of PSD-95 was identified in the 201–226 lane only. Purified GST fusion proteins were identified using Coomassie Blue staining (*right panel*). *F*, brain lysates were pulled down with GST-wild type (QSPK) or GST-S224A point mutant (QAPK). Note that S224A mutant failed to bind PSD-95, whereas the wild type strongly binds to PSD-95. Purified GST fusion proteins were identified using Coomassie Blue staining (*right panel*). *T*, transmembrane region.

the most conserved residue among various PDZ binding motifs (21). We found that the S224A mutant failed to bind PSD-95, whereas the wild type strongly binds to PSD-95 (Fig. 2*F*).

Interaction of calcyon with PSD-95 was further confirmed by immunocytochemistry. Neurons were doubly stained with calcyon and PSD-95 antibodies. Although calcyon was found to be present throughout the cytosol, it partially colocalized with PSD-95 in the dendritic spines (supplemental Fig. 3*A*). When exogenously expressed, calcyon also was found in the punctate structures, which were partially colocalized with the endosomal marker, EEA1, in the dendritic spines (supplemental Fig. 3*B*). Consistent with endogenous staining, exogenously expressed calcyon also exhibited partial colocalization with PSD-95 (supplemental Fig. 3*E*). We also found that calcyon was partially colocalized with various early endosome markers; early endosome antigen 1 protein (EEA1), double FYVE domain from the hepatocyte-growth-factor-regulated tyrosine kinase substrate (2XFYVE-Hrs) or transferrin-conjugated Texas Red in COS-7 cells (supplemental Fig. 4).

The N terminus of PSD-95 is known to interact with the C terminus of D_1DR (13). Although a direct interaction between calcyon and D_1DR turned out to be misinterpreted because our results indicated that calcyon and PSD-95 associate with each other, there is a possibility that calcyon and D_1DR interact indirectly through PSD-95 as a mediator. To test this possibility, we first incubated purified GST-calcyon or GST-only with HEK293T cell lysates that expressed HA-D_1DR and PSD-95-EGFP and immunoprecipitated with GST antibody followed by

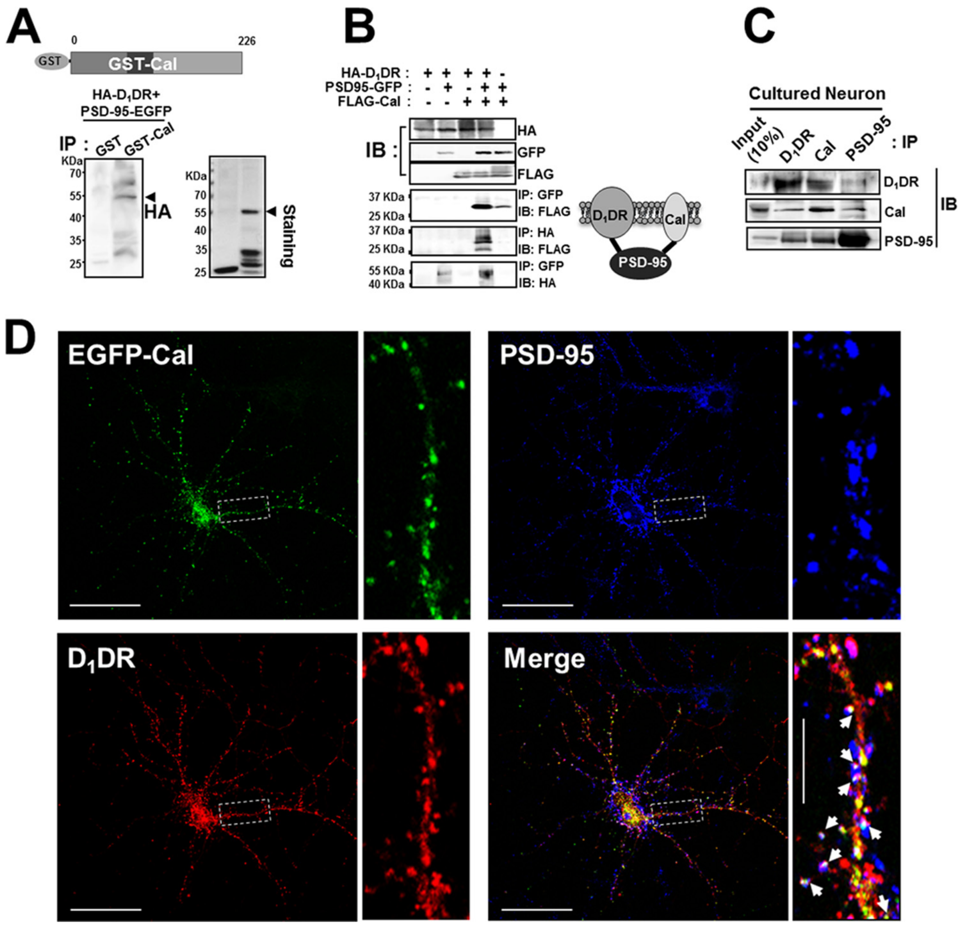

FIGURE 3. **Calcyon interacts indirectly with D$_1$DR via PSD-95.** *A*, HEK293T cells were cotransfected with EGFP-tagged PSD-95 and HA-tagged D$_1$DR, lysed, immunoprecipitated (*IP*) with GST or GST-calcyon (*GST-Cal*), and immunoblotted with anti-HA antibody. *Arrowhead* indicates HA-tagged D$_1$DR (*left panel*) and purified GST-calcyon wild type (*right panel*). Purified GST-calcyon was identified using Coomassie Blue staining (*right panel*). *B*, HEK293T cells were cotransfected with EGFP-tagged PSD-95, HA-tagged D$_1$DR, and FLAG-tagged calcyon. Cells were lysed, immunoprecipitated, and immunoblotted (*IB*) with various combinations of the indicated antibodies. Note that when only three proteins were cotransfected, calcyon was coimmunoprecipitated with D$_1$DR (*left panel*). *Right panel*), model depicting a putative molecular interaction of calcyon·PSD-95·D$_1$DR. *C*, endogenous complex of calcyon·PSD-95·D$_1$DR in the cultured neurons. The cultured primary hippocampal neurons (days *in vitro* 21) were incubated with 10 μM SKF-81297 for 15 min, lysed in RIPA buffer, immunoprecipitated, and immunoblotted with rabbit polyclonal anti-D$_1$DR, -calcyon, or -PSD-95 antibody. 10% neuron lysates (70 μg) were loaded as the positive control. *D*, D$_1$DR, PSD-95, and calcyon were colocalized in the dendritic spines and dendritic shaft. Because the antibody species matter, GFP-tagged calcyon was transfected, whereas PSD-95 and D$_1$DR were detected endogenously with mouse anti-PSD-95 antibody (secondary antibody Alexa Fluor 405-conjugated anti-mouse antibody) and rabbit anti-D$_1$DR antibody (secondary antibody Alexa Fluor 594-conjugated anti-rabbit antibody). *Arrows* indicate the spines where the calcyon·PSD-95·D$_1$DR complex was colocalized. *Scale bar* = 50 μm; *scale bar* = 10 μm in *inset*.

immunoblotting with HA-antibody. We found that HA-D$_1$DR was coimmunoprecipitated with GST-calcyon (Fig. 3*A*). Second, HEK293T cells were transfected with various combinations of HA-D$_1$DR, PSD-95-GFP, and FLAG-calcyon, and coimmunoprecipitation followed by immunoblotting with specific antibodies was carried out. PSD-95-GFP was coprecipitated with either FLAG-calcyon or HA-D$_1$DR when doubly transfected. Interestingly, HA-D$_1$DR and FLAG-calcyon only coprecipitated if PSD-95-GFP was triply cotransfected, strongly suggesting that PSD-95 acts as a linker between calcyon and D$_1$DR (Fig. 3*B*). Finally, we confirmed that a calcyon·PSD-95·D$_1$DR ternary complex exists endogenously in the brain by immunoprecipitation assay in cultured neurons after treatment with a D$_1$DR-specific agonist, SKF-81297 for 15 min. Immunoblot analysis with antibodies against each protein showed that calcyon, PSD-95, and D$_1$DR coprecipitated together (Fig. 3*C*). Immunocytochemistry also showed that the three proteins are colocalized in the dendritic spines, especially the spine heads (Fig. 3*D* and supplemental Fig. 5).

The D$_1$-like receptors activate cyclic AMP production and bidirectionally modulate protein kinase A (PKA) and DARPP-32 through $G_{s/olf}$ (24). Intriguingly, D$_1$DR-stimulated Ca^{2+} release was significantly attenuated by treatment with a PKC inhibitor in calcyon-expressing cells, and calcyon was found to be phosphorylated by purified PKC, although no detailed analysis has been done (2). We also found that calcyon was phosphorylated on the serine residue by the PKC activator PMA, and this phosphorylation was blocked by the PKC inhibitors GF109203X and rottlerin but not by the PKA inhibitor H-89 (Fig. 4*A*). We further investigated the specific phosphorylation sites of calcyon by PKC. Human calcyon is phosphorylated on Ser-154 and Ser-196 by PKA (2), whereas the rat calcyon has a putative PKC phosphorylation site on Ser-169 in the cytoplasmic domain (the NetPhosK 1.0 Server). HEK293T cells were transfected with an EGFP-tagged wild-type calcyon or S169A phospho-deficient mutant and incubated with PMA. Fig. 4*B* shows that the wild type, but not the S169A mutant, was rapidly phosphorylated on the serine residues by PMA, suggest-

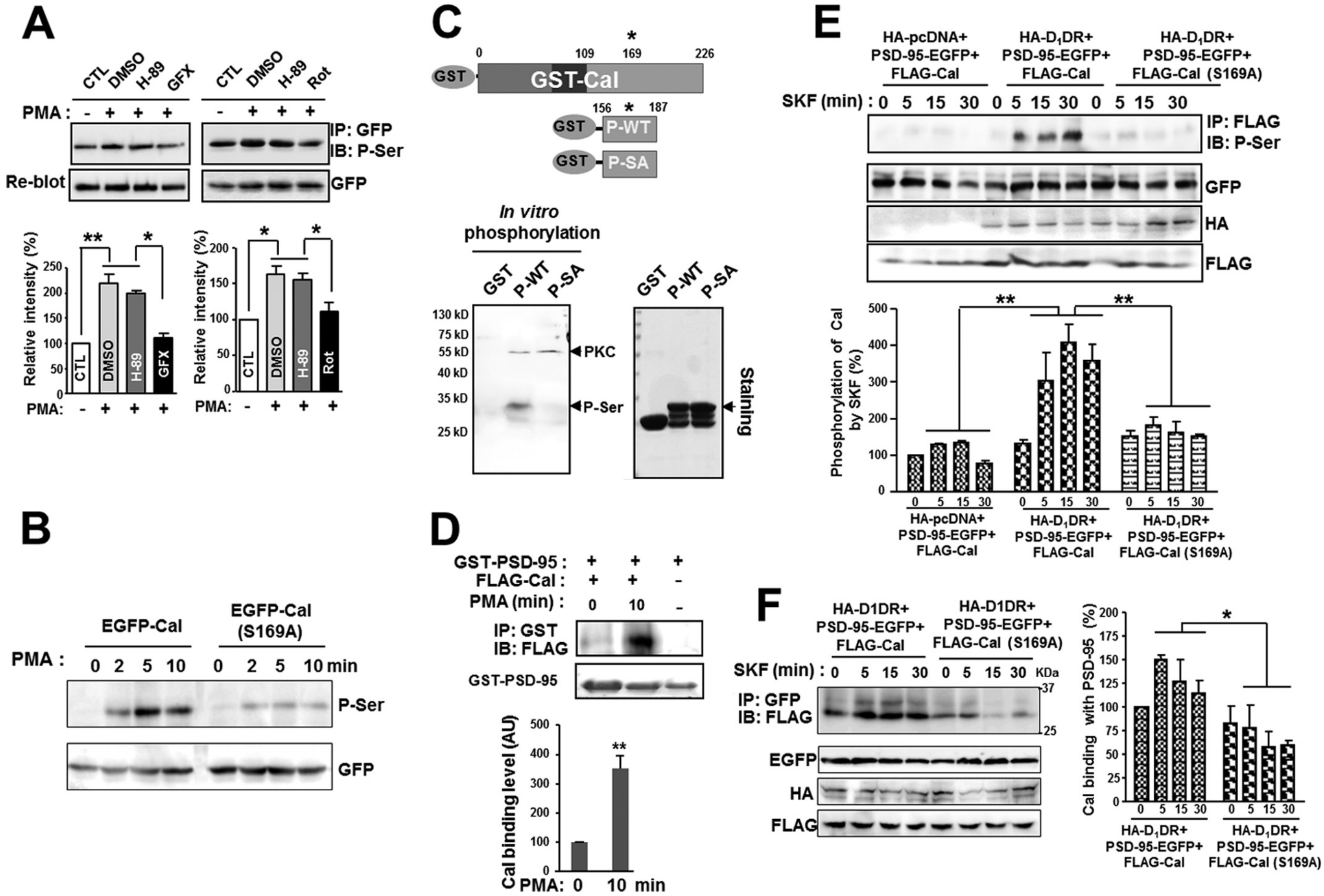

FIGURE 4. **Phosphorylation of calcyon by PKC enhances its interaction with PSD-95.** *A*, the phosphorylation of calcyon by PKC. HEK293T cells were transfected with EGFP-calcyon and preincubated with DMSO and 20 μM H-89 (PKA inhibitor) for 20 min or two different PKC inhibitors, 5 μM GF109203X (*GFX*) for 45 min and 30 μM rottlerin (*Rot*) for 30 min. After preincubation, cells were treated with 1 μM PMA, a PKC activator, for 10 min, harvested, and coimmunoprecipitated with anti-GFP antibody followed by immunoblotting with anti-phospho-serine antibody. *Lower bar graphs*: quantification from three independent experiments. Data are the mean $\pm$ S.E. *Asterisks* indicate a significant change when compared with the group(s) indicated (one-way ANOVA; *, $p < 0.05$, **, $p < 0.01$). *CTL*, control. *B*, HEK293T cells expressing EGFP-calcyon (*EGFP-Cal*) or phospho-deficient mutant EGFP-calcyon (S169A) (*EGFP-Cal (S169A)*) were incubated with PMA for the indicated times and coimmunoprecipitated with anti-GFP antibody followed by immunoblotting with phospho-serine (*P-Ser*) antibody. *C*, purified GST-tagged wild type (*P-WT*) and phospho-deficient mutant S169A (*P-SA*) of calcyon were incubated with the PKC catalytic subunit in the presence of ATP. The phosphorylation was analyzed by SDS-PAGE and immunoblotting with phospho-serine antibody (*left panel*). *Arrowheads* indicate the PKC catalytic subunit and phosphorylated serine. Purified GST fusion proteins were identified using Coomassie Blue staining (*right panel*). *D*, HEK293T cells expressing FLAG-calcyon were incubated with 1 μM PMA for 10 min, and lysates were coprecipitated with GST-PSD-95 beads and immunoblotted with anti-FLAG antibody. The amount of FLAG-calcyon pulled down with GST-PSD-95 increased more than 3-fold after treatment with PMA for 10 min. Statistical analysis was performed using Student's *t* test. **, $p < 0.01$. *AU*, arbitrary units. *E*, HA-D$_1$DR·PSD-95-EGFP and FLAG-calcyon or FLAG-calcyon (S169A) were cotransfected into HEK293T cells. After treatment with SKF-81297 for the indicated times, cells were lysed and immunoprecipitated with anti-FLAG antibody followed by immunoblotting with phospho-serine antibody. Note that in the absence of HA-D$_1$DR expression, SKF-81297 treatment failed to induce the phosphorylation of calcyon. *Lower graph*: quantification from three independent experiments. *Asterisks* indicate significant changes in the second group when compared with the first and the third group at matching time points. ANOVA and Tukey's HSD post hoc test; **, $p < 0.01$. *F*, HA-D1DR·PSD-95-EGFP and FLAG-calcyon or FLAG-calcyon (S169A) were cotransfected into HEK293T cells. After treatment of SKF-81297 for the indicated times, cells were lysed and immunoprecipitated with anti-GFP antibody followed by immunoblotting with anti-FLAG antibody. Phosphorylation of calcyon by SKF-81297 increased its interaction with PSD-95. *Asterisk* indicates significant changes in the second group when compared with the first group at matching time points. ANOVA and Tukey's HSD post hoc test; *, $p < 0.05$.

ing that Ser-169 is the major phosphorylation site of calcyon by PKC. This was further confirmed by an *in vitro* phosphorylation assay (Fig. 4*C*). We purified a.a 156–187 from wild type (P-WT) and the phospho-deficient mutant S169A (P-SA) of calcyon and incubated them with the purified PKC catalytic subunit in the presence of ATP. Phosphorylation on the serine residues was observed in the P-WT but not in the P-SA, suggesting that calcyon is directly phosphorylated by PKC on Ser 169 (Fig. 4*C*).

We next tested whether the phosphorylation of calcyon modulates its interaction with PSD-95. HEK293T cells were transfected with FLAG-calcyon and incubated with 1 μM PMA for 10 min. Then, the lysates were precipitated with purified GST-PSD-95 beads and immunoblotted with FLAG-antibodies. Fig. 4*D* shows that the interaction between calcyon and PSD-95 was dramatically increased by treatment with PMA. Interestingly, calcyon was also phosphorylated on the serine residues after SKF-81297 treatment, whereas the S169A mutant was not (Fig. 4*E*). Direct activation of PKC by PMA resulted in a maximum increase of calcyon phosphorylation only 5 min after treatment (Fig. 4*B*), whereas SKF-81279 treatment induced maximum calcyon phosphorylation 15 min after

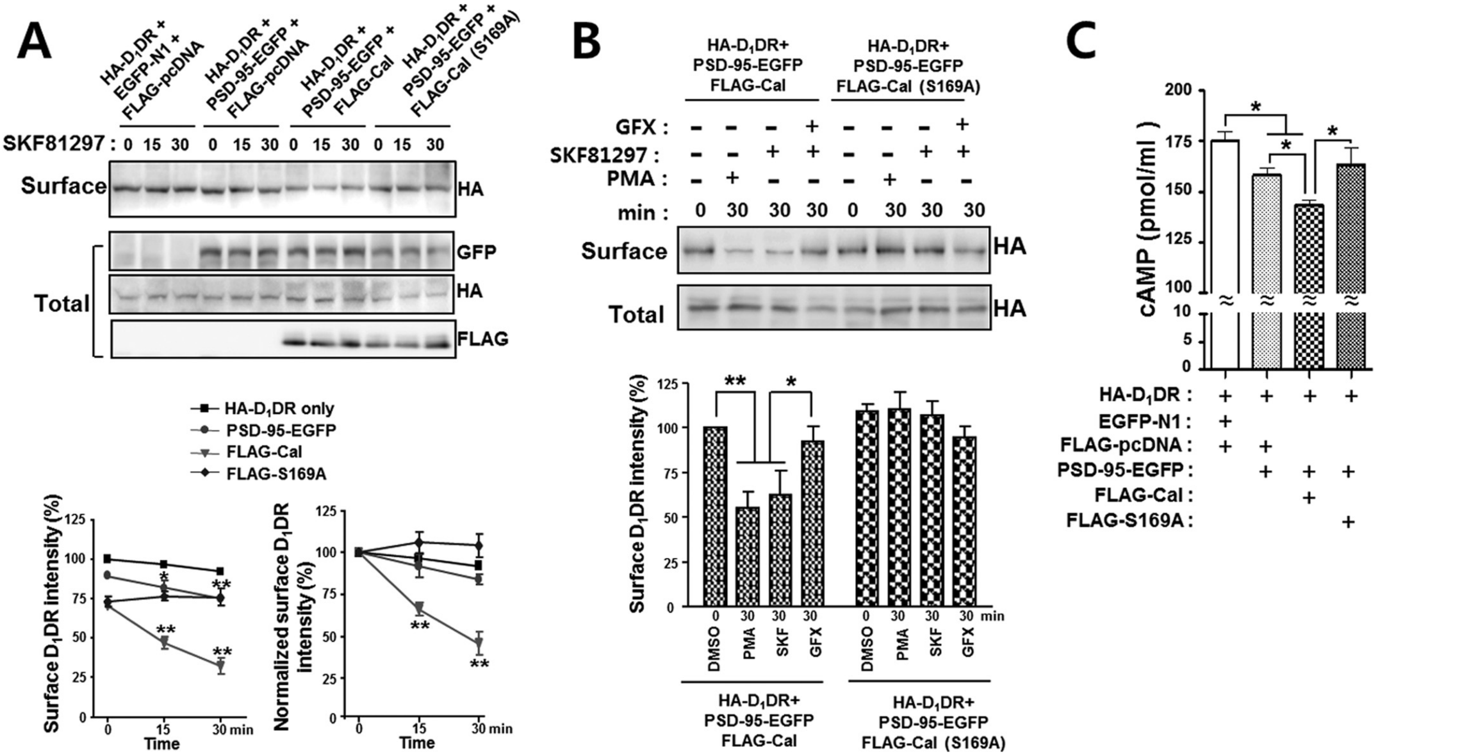

FIGURE 5. **The phosphorylation of calcyon and the internalization of the surface D_1DR are tightly correlated.** *A*, HEK293T cells were transfected with various combinations of constructs as indicated. Cells were then exposed to 10 μM SKF-81297 for the indicated times, and surface biotinylation experiments were performed as described under "Experimental Procedures." The surface levels of D_1DR were gradually decreased after SKF-81297 treatments in cells coexpressing D_1DR and PSD-95 or D_1DR, PSD-95 and calcyon, although when the three proteins were coexpressed, the rate of decrease was much faster. The phospho-deficient mutant of calcyon (S169A) failed to induce D_1DR internalization after treatment with SKF-81297. *Lower graphs*: quantification from five independent experiments (*left graph*). The surface intensity values of D_1DR at the indicated times were normalized to the that at time 0 to emphasize the rate of internalization of surface D_1DR after SKF-81297 treatment (*right graph*). *Asterisks* indicate significant changes in each group when compared with the HA-D_1DR group at matching time points. ANOVA and Tukey's HSD post hoc test; *, $p < 0.05$, **, $p < 0.01$. *B*, HEK293T cells expressing the FLAG-calyon (*FLAG-Cal*) or FLAG-calcyon (S169A) with HA-D1DR·PSD-95-EGFP were incubated with 10 μM SKF-81297 or 1 μM PMA for 30 min in the presence or absence of 5 μM GF109203X (*GFX*). Surface biotinylation experiments were performed, and surface as well as total levels of D_1DRs were measured by immunoblotting with anti-HA antibody. The intensity of surface biotinylated proteins was normalized to the total protein intensity. *Lower graphs*: quantification from three independent experiments. *Asterisks* indicate significant changes in the PMA- or SKF-81297-treated group when compared with the DMSO-treated group or GF109203X-treated group. Data represent the mean ± S.E. ANOVA and Tukey's HSD post hoc test; *, $p < 0.05$, **, $p < 0.01$. *C*, HEK293T cells were transfected with the same constructs as in *A*. Cells were then exposed to 10 μM SKF-81297 for 30 min, and cAMP direct immunoassays were performed as described under "Experimental Procedures." The SKF-81297-induced cAMP accumulation levels were significantly diminished in cells coexpressing D_1DR, PSD-95, and calcyon when compared with D_1DR or D_1DR with PSD-95. The data are means ± S.E. from at least three independent experiments. *Asterisks* indicate significant changes between linked groups. ANOVA and Tukey's HSD post hoc test; *, $p < 0.05$.

treatment (Fig. 4*E*), suggesting that D_1DR activation by SKF-81297 indirectly causes PKC activation during D_1DR signal transduction. Consistently, SKF-81297 treatment significantly increased the interaction of PSD-95 with calcyon but not with the S169A mutant (Fig. 4*F*).

PSD-95 interacts with D_1DR, promoting the internalization of the surface D_1DR (13). Thus, we next investigated whether calcyon could regulate the internalization of the surface D_1DR through the ternary complex with PSD-95. HEK293T cells were triply cotransfected with HA-D_1DR, PSD-95-EGFP, and the FLAG-calcyon or FLAG-S169A mutant. The surface biotinylation assay showed that the surface level of D_1DR rapidly decreased after treatment with SKF-81297 in the presence of calcyon. When compared with the D_1DR only or D_1DR with PSD-95 groups, when calcyon was cotransfected with D_1DR and PSD-95, the slope of the decrease was much steeper (Fig. 5*A*). The phospho-deficient S169A mutant of calcyon failed to induce D_1DR internalization after treatment with SKF-81297 (Fig. 5*A*).

To further test whether the decrease in the surface level of D_1DR depends on the phosphorylation of calcyon, triply cotransfected HEK293T cells were incubated with 10 μM SKF-81297, 1 μM PMA, or 5 μM GF109203X, and the surface levels of D_1DR were measured. Fig. 5*B* shows that both PMA and SKF-81297 treatments induced significant decreases in the surface level of D_1DR, whereas GF109203X treatment did not. Evidently, the S169A mutant did not induce any significant changes in the surface levels of D_1DR after treatment with PMA, SKF-81297, or GF109203X (Fig. 5*B*). To test whether the formation of the ternary complex has an effect on D_1DR-mediated signaling, HEK293T cells were transfected with various combinations of constructs, and after incubation with 10 μM SKF-81297 for 30 min, cAMP levels were measured (Fig. 5*C*). We found that in the presence of calcyon, PSD-95, and D_1DR, SKF-81297-stimulated cAMP production was significantly reduced when compared with D_1DR only or PSD-95 with D_1DR. The phospho-deficient mutant of calcyon (S169A) failed to affect cAMP production. Because the interaction between calcyon and PSD-95 increased by the phosphorylation of calcyon, our results suggest that D_1DR activation by SKF-81297 induces the PKC-mediated phosphorylation of calcyon, which promotes the formation of a ternary complex between calcyon and D_1DR through PSD-95 and consequently induces the internalization of D_1DR, thus inhibiting D_1DR signaling.

Previously, calcyon and D_1DR were thought to interact with each other, but later on, it was discovered there was no direct interaction between them (8). Growing evidence, however, indicates that calcyon has important roles in D_1DR-mediated signaling pathways as well as in various D_1DR-related neuropsychiatric disorders (4, 5, 25–27). Therefore, it was widely assumed that calcyon could interact with D_1DR either functionally or indirectly. D_1DR is regulated by the glutamatergic scaffolding protein PSD-95 through direct interaction, which facilitates the constitutive internalization of D_1DR as well as the internalization of the NMDA receptor that complexes with D_1DR (15). In addition, D_1DR interacts with NMDA receptor and balances NMDA receptor-mediated responses through both a PKA-dependent pathway and a Ca^{2+}-dependent mechanism (28). Furthermore, recent studies revealed that calcyon is required for the NMDA activity-dependent internalization of AMPA receptor, which leads to long-term depression (29). All of these results imply that there could be many possible interactions involving D_1DR, calcyon, and glutamate receptors. In the present study, we showed that calcyon forms a novel ternary complex with D_1DR through PSD-95, thus linking calcyon to D_1DR.

The PDZ homology domain is the most abundant protein interacting domain, and greater than 500 PDZ domains have been identified in eukaryotic cells so far (30). The PDZ1 domain of PSD-95 is known to interact with GluR6, the C terminus of the NMDA receptor NR2 subunits, and the C terminus of the Kir2.1 and Kv1.4 potassium channels (31–34). There are no reports as to whether rat calcyon has the PDZ binding motif, but we found that the last four-amino acid sequence (QSPK) of calcyon mediates the interaction with the PDZ-1 domain of PSD-95 (Fig. 2*E* and supplemental Fig. 2, *B* and *C*). Therefore, calcyon may compete with other proteins for binding to PSD-95, which subsequently affects the signaling pathways downstream to these proteins, although this requires further detailed study.

Human calcyon is predicted to be phosphorylated by PKC, although direct evidence has not been provided (2). We found that rat calcyon contains eight putative phosphorylation sites, but the Ser-169 residue is a unique site that can be phosphorylated by PKC. Indeed, the phospho-deficient mutant S169A largely failed to be phosphorylated by the PKC activator PMA (Fig. 4*B*). Interestingly, the D_1DR-specific agonist SKF-81297 also increased the phosphorylation levels of wild-type calcyon but not those of the S169A mutant, indicating that the D_1DR signaling pathway may activate PKC either directly or indirectly to phosphorylate calcyon.

PKC-mediated phosphorylation of calcyon does affect its binding to PSD-95. As the phosphorylation level of calcyon increases, the binding to PSD-95 increases. Because PSD-95 is known to bind D_1DR, the phosphorylation of calcyon by PKC possibly enhances the formation of the ternary complex of calcyon·PSD-95·D_1DR. What is the consequence of forming this ternary complex? We showed that phosphorylation of calcyon increased the internalization of D_1DR from the cell surface. Thus, we could speculate about the existence a possible feedback loop during D_1DR signaling. D_1DR is activated by its agonist followed by signaling to its downstream effectors, which activates PKC that subsequently phosphorylates calcyon. The phosphorylated calcyon binds more strongly to PSD-95 and is recruited to the cell surface either by its binding to PSD-95 or by other unknown mechanisms and forms a ternary complex with PSD-95 and D_1DR, which consequently induces the internalization of D_1DR from the cell surface (supplemental Fig. 6). Our data imply that the formation of the calcyon·PSD-95·D_1DR complex in dendritic spines would indirectly inhibit D_1DR-mediated signaling by "physically" reducing the surface levels of D_1DR and thus may provide a novel target for D_1DR-related neuropsychiatric diseases such as schizophrenia and attention deficit hyperactivity disorder. Whether the phosphorylation-dependent formation of a ternary complex among calcyon·PSD-95·D_1DR directly affects D_1DR-mediated signaling and plays a role in linking dopaminergic and glutamatergic signaling in the brain would be of great interest but certainly requires further investigation.

Acknowledgment—Microscopic data for this study were acquired and analyzed in the Biomedical Imaging Center at the Seoul National University College of Medicine.

REFERENCES

1. Lezcano, N., and Bergson, C. (2002) D_1/D_5 dopamine receptors stimulate intracellular calcium release in primary cultures of neocortical and hippocampal neurons. *J. Neurophysiol.* **87,** 2167–2175
2. Lezcano, N., Mrzljak, L., Eubanks, S., Levenson, R., Goldman-Rakic, P., and Bergson, C. (2000) Dual signaling regulated by calcyon, a D_1 dopamine receptor interacting protein. *Science* **287,** 1660–1664
3. Lezcano, N., Mrzljak, L., Levenson, R., and Bergson, C. (2006) Retraction. *Science* **314,** 1681
4. Koh, P. O., Bergson, C., Undie, A. S., Goldman-Rakic, P. S., and Lidow, M. S. (2003) Up-regulation of the D_1 dopamine receptor-interacting protein, calcyon, in patients with schizophrenia. *Arch. Gen. Psychiatry* **60,** 311–319
5. Clinton, S. M., Ibrahim, H. M., Frey, K. A., Davis, K. L., Haroutunian, V., and Meador-Woodruff, J. H. (2005) Dopaminergic abnormalities in select thalamic nuclei in schizophrenia: involvement of the intracellular signal integrating proteins calcyon and spinophilin. *Am. J. Psychiatry* **162,** 1859–1871
6. Trantham-Davidson, H., Vazdarjanova, A., Dai, R., Terry, A., and Bergson, C. (2008) Up-regulation of calcyon results in locomotor hyperactivity and reduced anxiety in mice. *Behav. Brain Res.* **189,** 244–249
7. Vazdarjanova, A., Bunting, K., Muthusamy, N., and Bergson, C. (2011) Calcyon up-regulation in adolescence impairs response inhibition and working memory in adulthood. *Mol. Psychiatry* **16,** 672–684
8. Heijtz, R. D., Alexeyenko, A., and Castellanos, F. X. (2007) Calcyon mRNA expression in the frontal-striatal circuitry and its relationship to vesicular processes and ADHD. *Behav. Brain Funct.* **3,** 33
9. Luo, X., Kranzler, H., Lappalainen, J., Rosenheck, R., Charney, D., Zuo, L., Erdos, J., van Kammen, D. P., and Gelernter, J. (2004) *CALCYON* gene variation, schizophrenia, and cocaine dependence. *Am. J. Med. Genet. B Neuropsychiatr. Genet.* **125B,** 25–30
10. Lidow, M. S., Roberts, A., Zhang, L., Koh, P. O., Lezcano, N., and Bergson, C. (2001) Receptor cross-talk protein, calcyon, regulates affinity state of dopamine D_1 receptors. *Eur. J. Pharmacol.* **427,** 187–193

11. Xiao, J., Dai, R., Negyessy, L., and Bergson, C. (2006) Calcyon, a novel partner of clathrin light chain, stimulates clathrin-mediated endocytosis. *J. Biol. Chem.* **281,** 15182–15193
12. Cho, K. O., Hunt, C. A., and Kennedy, M. B. (1992) The rat brain postsynaptic density fraction contains a homolog of the *Drosophila* discs-large tumor suppressor protein. *Neuron* **9,** 929–942
13. Zhang, J., Vinuela, A., Neely, M. H., Hallett, P. J., Grant, S. G., Miller, G. M., Isacson, O., Caron, M. G., and Yao, W. D. (2007) Inhibition of the dopamine D_1 receptor signaling by PSD-95. *J. Biol. Chem.* **282,** 15778–15789
14. Sun, P., Wang, J., Gu, W., Cheng, W., Jin, G. Z., Friedman, E., Zheng, J., and Zhen, X. (2009) PSD-95 regulates D_1 dopamine receptor resensitization, but not receptor-mediated G_s-protein activation. *Cell Res.* **19,** 612–624
15. Zhang, J., Xu, T. X., Hallett, P. J., Watanabe, M., Grant, S. G., Isacson, O., and Yao, W. D. (2009) PSD-95 uncouples dopamine-glutamate interaction in the D_1·PSD-95·NMDA receptor complex. *J. Neurosci.* **29,** 2948–2960
16. Hallett, P. J., Collins, T. L., Standaert, D. G., and Dunah, A. W. (2008) Biochemical fractionation of brain tissue for studies of receptor distribution and trafficking. *Curr. Protoc. Neurosci.* Chapter 1, Unit 1 16
17. Chang, S., and De Camilli, P. (2001) Glutamate regulates actin-based motility in axonal filopodia. *Nat. Neurosci.* **4,** 787–793
18. Xia, Z., Dudek, H., Miranti, C. K., and Greenberg, M. E. (1996) Calcium influx via the NMDA receptor induces immediate early gene transcription by a MAP kinase/ERK-dependent mechanism. *J. Neurosci.* **16,** 5425–5436
19. Kim, E., and Sheng, M. (2004) PDZ domain proteins of synapses. *Nat. Rev. Neurosci.* **5,** 771–781
20. Kennedy, M. B. (2000) Signal-processing machines at the postsynaptic density. *Science* **290,** 750–754
21. Kerppola, T. K. (2006) Design and implementation of bimolecular fluorescence complementation (BiFC) assays for the visualization of protein interactions in living cells. *Nat. Protoc.* **1,** 1278–1286
22. Morell, M., Espargaro, A., Aviles, F. X., and Ventura, S. (2008) Study and selection of *in vivo* protein interactions by coupling bimolecular fluorescence complementation and flow cytometry. *Nat. Protoc.* **3,** 22–33
23. Shyu, Y. J., Liu, H., Deng, X., and Hu, C. D. (2006) Identification of new fluorescent protein fragments for bimolecular fluorescence complementation analysis under physiological conditions. *BioTechniques* **40,** 61–66
24. Greengard, P., Allen, P. B., and Nairn, A. C. (1999) Beyond the dopamine receptor: the DARPP-32/protein phosphatase-1 cascade. *Neuron* **23,** 435–447
25. Heijtz, R. D., Kolb, B., and Forssberg, H. (2007) Motor inhibitory role of dopamine D_1 receptors: implications for ADHD. *Physiol. Behav.* **92,** 155–160
26. Thompson, D., Martini, L., and Whistler, J. L. (2010) Altered ratio of D_1 and D_2 dopamine receptors in mouse striatum is associated with behavioral sensitization to cocaine. *PLoS One* **5,** e11038
27. Durstewitz, D., and Seamans, J. K. (2002) The computational role of dopamine D_1 receptors in working memory. *Neural Netw.* **15,** 561–572
28. Wang, J., and O'Donnell, P. (2001) D_1 dopamine receptors potentiate NMDA-mediated excitability increase in layer V prefrontal cortical pyramidal neurons. *Cereb. Cortex* **11,** 452–462
29. Davidson, H. T., Xiao, J., Dai, R., and Bergson, C. (2009) Calcyon is necessary for activity-dependent AMPA receptor internalization and LTD in CA1 neurons of hippocampus. *Eur. J. Neurosci.* **29,** 42–54
30. Feng, W., and Zhang, M. (2009) Organization and dynamics of PDZ domain-related supramodules in the postsynaptic density. *Nat. Rev. Neurosci.* **10,** 87–99
31. Sornarajah, L., Vasuta, O. C., Zhang, L., Sutton, C., Li, B., El-Husseini, A., and Raymond, L. A. (2008) NMDA receptor desensitization regulated by direct binding to PDZ1–2 domains of PSD-95. *J. Neurophysiol.* **99,** 3052–3062
32. Hu, S. Q., Zhu, J., Pei, D. S., Zong, Y. Y., Yan, J. Z., Hou, X. Y., and Zhang, G. Y. (2009) Overexpression of the PDZ1 domain of PSD-95 diminishes ischemic brain injury via inhibition of the GluR6·PSD-95·MLK3 pathway. *J. Neurosci. Res.* **87,** 3626–3638
33. Pegan, S., Tan, J., Huang, A., Slesinger, P. A., Riek, R., and Choe, S. (2007) NMR studies of interactions between C-terminal tail of Kir2.1 channel and PDZ1,2 domains of PSD-95. *Biochemistry* **46,** 5315–5322
34. Imamura, F., Maeda, S., Doi, T., and Fujiyoshi, Y. (2002) Ligand binding of the second PDZ domain regulates clustering of PSD-95 with the Kv1.4 potassium channel. *J. Biol. Chem.* **277,** 3640–3646